Siyang Zhou

Titanium Isotope Fractionation During Multicomponent Diffusion in Molten Basalts

submitted in partial fulfillment of the requirements for the degree of
Master of Science in Earth and Environmental Sciences
Department of Earth and Environmental Sciences
The University of Michigan

Accepted by:

Youxue Zhang	Signature	Youxue Zhang	Name / Date: 7/10/2023
Jie Li	Signature (Digitally signed by Jie Li Date: 2023.07.14 09:26:45 -04'00')		Name / Date
	Department Chair Signature	Julia Cole	Name / Date: 7/31/23

I hereby grant the University of Michigan, its heirs and assigns, the non-exclusive right to reproduce and distribute single copies of my thesis, in whole or in part, in any format. I represent and warrant to the University of Michigan that the thesis is an original work, does not infringe or violate any rights of others, and that I make these grants as the sole owner of the rights to my thesis. I understand that I will not receive royalties for any reproduction of this thesis.

☒ Permission granted.

☐ Permission granted to copy after: _____

☐ Permission declined.

Siyang Zhou
Author Signature

Earth and Environmental Sciences
UNIVERSITY OF MICHIGAN

Siyang Zhou

syzhoupd@umich.edu

© Siyang Zhou 2023

Acknowledgements

This research was supported by NSF grant EAR-2020603. Throughout the whole study time in graduate school and the thesis writing process, I really appreciate the guidance from Prof. Youxue Zhang. His professional and enlightening suggestions solve my plenty of problems on academy. I am also highly grateful for his patience when I meet long-term mental health problem in the second year. Thanks very much to Prof. Noriko. K. Tita to analyze samples and provide high quality data for this study. Meanwhile, thanks to Dr. Owen Neil and Zhengjiu Xu about technical help all the time.

Table of Contents

List of Tables

List of Figures

Abstract

This thesis reports the first study of diffusive Ti isotope fractionation in haplobasaltic melts using diffusion couple experiments. The experimental charges are from Guo and Zhang (2016). The $^{49}Ti/^{47}Ti$ isotope ratio profiles in diffusion couple experiments have been measured by Secondary Ion Mass Spectrometry (SIMS). We pushed the limits of current SIMS to measure non-traditional stable isotope ratio. The resulting data show that SIMS measurements using IMS-1280 can reach 0.10‰ (2σ) with effort at TiO_2 concentration of ~3 wt% using multi-collection Faraday cup. For initial Ti concentration contrast of about 200 in a diffusion couple, the total variation in $^{49}Ti/^{47}Ti$ across a diffusion couple profile is about 3.2‰. By fitting the isotope ratio profiles, the β value is 0.030 ± 0.002 for the MgO-TiO_2 interdiffusion couples and 0.036 ± 0.004 for the SiO_2-TiO_2 interdiffusion couples both at 1500°C. Hence, the total Ti isotope ratio variation would be > 1‰ along a diffusion profile when the initial TiO_2 concentration contrast between two diffusion species is larger than 15. Such high concentration contrast may be realized for basalt-rhyolite magma mixing. These results will expand the database of diffusion parameters for non-traditional isotopes and provide new insight into Ti isotope fractionation during magma process, with potential to further understand magma revolution.

Chapter 1 Introduction

Isotope fractionation during diffusion is a fundamental process in magma systems during mineral growth/dissolution (e.g., Jambon, 1980; Watkins et al., 2017), and magma mixing and interaction (e.g., Chopra et al., 2012). Although diffusion tends to reduce concentration gradients, interestingly it may lead to significant isotope separation in an initially isotopically homogeneous system with concentration gradients, which makes observing and measuring diffusive isotope fractionation possible.

1.1 Theoretical background

Isotope fractionation during diffusion is due to diffusivity difference for different isotopes. The difference is too small to be resolved by directly measuring diffusivities of individual isotopes. Therefore, isotope ratio profiles are used to determine the ratio of diffusivities of different isotopes. Theoretically, diffusivity ratio is related to the mass ratio of different isotopes because the heavier isotope always diffuses at a slower speed. If each isotope diffuses freely as individual neutral atoms, diffusivities of heavy and light isotopes can be related by gas dynamic theory leading to Graham's law (Richter et al., 2003):

$$D_H/D_L = (m_L/m_H)^{1/2}, \quad (1)$$

where D_{H} and D_{L} are the diffusivities of the heavier isotope and lighter isotope, m_H and m_L are the atomic masses of the heavy and light isotopes. If heavy and light isotopes diffuse freely as individual neutral molecules, then:

$$D_H/D_L = (M_L/M_H)^{1/2}, \quad (2)$$

where M_H and M_L are the molecular masses of the molecules containing heavy and light isotopes.

In magma system, diffusion often involves clusters and exchange, Richter et al (2006) gives the theoretical equation for diffusivity ratio between two different isotopes in this case:

$$D_H/D_L = \left[\frac{M_L(M_H+M)}{M_H(M_L+M)}\right]^{1/2}, \quad (3)$$

where M_H and M_L are the masses of the clusters containing heavy and light isotopes, and M is the mass of the counter-diffusing species, which are species diffusing in the opposite direction with the investigated element considering mass conservation of the whole system.

However, silicate melts are complicated in structure and particle motions, making the diffusion species and mechanisms unknown. Hence, an empirical approach is used to characterize the relation between two different isotopes as follows (Richter et al., 1999):

$$D_H/D_L = (m_L/m_H)^{\beta}, \quad (4)$$

where β is an empirical parameter characterizing the diffusivity difference between heavy and light isotopes. Considering Eqs.1, 2 and 3, we could obtain that $0 \leq \beta \leq 0.5$ (Zhang et al., 2022).

1.2 Literature review

Richter et al. (1999) reported the first diffusive isotope fractionation analysis result for Ca in CaO-SiO_2-Al_2O_3 system, which is much simpler than natural magma composition. They used $CaCO_3$ with special isotope abundance (from Oak Ridge National Laboratory) adding in this system to obtain higher initial $^{48}Ca/^{44}Ca$ ratio. The reason to choose Ca as the first element is

because it has relatively larger mass difference between the heaviest isotope and the lightest isotope, which can increase the isotope ratio's variation to obtain high quality data with SIMS. The results showed the β_{Ca} factor is from 0.05 to 0.1 at 1500°C. To further investigate diffusive isotope fractionation on natural element and isotope composition, Richter et al. (2003) used diffusion couple between basalt and rhyolite for Li and Ca. Li has larger diffusivity and isotope fractionation; therefore, $^{7}Li/^{6}Li$ ratio was measured by SIMS, however, the $^{44}Ca/^{40}Ca$ ratio variation in natural sample cannot be resolved by SIMS at that time because it is too small. To solve this problem, they cut diffusion couples perpendicular to their long axis into a series of 'boards' about 0.5 mm thick and measured the $^{44}Ca/^{40}Ca$ of each board using thermal ionization mass spectrometry (TIMS). By fitting the isotope profile, they obtained $\beta_{Li} \approx 0.215$ and $\beta_{Ca} \approx 0.075$ at about 1400°C.

Based on the idea and method developed above, there are large amounts of diffusive isotope fractionation data and parameter has been reported, enriching the database. For major element on magma system, the isotope ratio variation still cannot be resolved by SIMS in this time, the method for Ca on Richter et al. (2003) is continuously used. Continuously on basalt-rhyolite diffusion couples, Richter et al., (2008) showed $\beta_{Mg} = 0.05$ at 1400°C and Richter et al., (2009a) gave $\beta_{Fe} = 0.03$ at 1500°C. Watkins et al., (2009) investigated other kinds of diffusion couple and obtained $\beta_{Mg} \approx 0.10$ and $\beta_{Ca} \approx 0.165$ for molten albite-diopside couple, $\beta_{Ca} \approx 0.21$ for molten albite-anorthite couple all at 1450°C. For Li and Cl, the SIMS method was used and receive good data, for example, $\beta_{Cl} = 0.09 \pm 0.02$ for a molten dacite (Fortin et al., 2017), and $\beta_{Li} = 0.228$ in a wet rhyolite melt (Holycross et al., 2018).

Recently, Zhang (2022) used microbeam SIMS measurements on K isotope diffusive fractionation and obtained that β_K increased from 0.104±0.003 at 1260°C to 0.116±0.003 at

1500°C in basaltic SiO_2-K_2O interdiffusion couples, and slightly smaller in MgO-K_2O diffusion couples. This study gives us confidence to expand SIMS method to other major elements on magma system.

1.3 Ti diffusive isotope fractionation

Titanium is one of the major elements on silicate magma system. However, there has been no research on diffusive isotope fractionation of Ti. Whether diffusive Ti isotope fractionation is observable in natural magmatic processes is unknown. Here, we report the first study of diffusive Ti isotope fractionation in basaltic melts measured by SIMS. The result will allow us to quantify the transport of Ti isotopes and help us to gain a deeper understanding of the diffusion mechanism on molecular level. We will also evaluate some interesting Ti isotope data from natural samples. Moreover, diffusive fractionation of Ti isotopes to indicate thermal history with the combination of element diffusion and other isotope diffusion data, showing the formation and evolution process, especially for Ti-rich magma and Ti-related ore deposits.

Chapter 2 Method

2.1 Sample selection

Two diffusion couples with large TiO_2 concentration contrast were chosen for this study from Guo and Zhang (2016), where details of the experiments are described. Here is some specific information. Starting glasses of the diffusion halves were synthesized using reagent chemicals and their compositions are listed in Table.1. The compositional variation in terms of absolute concentrations is small, no more than 3 wt% for each oxide. In preparing the low-Ti concentration side (HB11 and HB17), no TiO_2 was added, which means TiO_2 in that half of the diffusion couple is from impurities in the reagent chemicals. Temperature and pressure condition of these two experiments are ~1500◦C and ~1GPa. HB11&12F has initial compensating concentration gradients mainly in SiO_2 and TiO_2, which is referred to as Si-Ti interdiffusion couples. Another couple (HB17&18A) has initial compensating concentration gradients mainly in MgO and TiO_2, which is referred to as Mg-K interdiffusion couples. The two series are used to examine the effect of the counter-diffusing oxide on the value of the empirical parameter β defined before (Eq.4).

Table.1 Average compositions (in wt%) of sample glasses in diffusion couples, 1σ uncertainty.

	SiO_2^* Ave(σ)	TiO_2 Ave(σ)	Al_2O_3 Ave(σ)	MgO Ave(σ)	CaO Ave(σ)	Na_2O Ave(σ)	K_2O Ave(σ)	Total
HB11	51.71(16)	0.02(2)	15.88(10)	9.62(07)	18.60(04)	2.66(2)	1.51(2)	100
HB12	49.25(15)	2.91(5)	16.06(08)	9.68(07)	18.07(72)	2.59(2)	1.44(2)	100
HB17	50.41(11)	0.02(2)	15.86(09)	11.10(07)	18.76(06)	2.40(2)	1.45(2)	100
HB18	50.44(15)	2.95(7)	15.61(08)	8.21(06)	18.61(08)	2.65(3)	1.53(2)	100

Note: Data are from Guo and Zhang, 2016, and SiO_2^* is defined as SiO_2 – (total – 100) from original EMPA data; therefore, the 'total' in this table are all 100%.

2.2 SIMS method

Preliminary measurement of Ti isotope ratios using Cameca IMS 7f GEO SIMS at Caltech did not provide good enough data. Hence, the decision and arrangement were made to use IMS 1280 at the University of Wisconsin-Madison. The Ti isotope ratios ($^{49}Ti/^{47}Ti$) analyzed using Cameca IMS 1280 at University of Wisconsin-Madison in this study have much better precision and consistency. Before sample analysis, we firstly proceeded test analysis using literature standard sample. Considering the test result and the feature of our samples, we did some innovations on the SIMS method compared to $^{41}K/^{39}K$ analyses (Zhang, 2022) and preliminary $^{49}Ti/^{47}Ti$ analyses at Caltech:

(1) We used three instrumental settings (sessions S1, S2, and S3, spots shown in Fig.1) to scan the sample to get higher quality data. S1 and S2 used single collector electron multiplier (EM) by magnetic field scan for low concentration side, while S3 used multi-collector Faraday cups (FC) with 10^{12} ohm feedback resistors for high concentration side. In all conditions, primary O^- ions from RF plasma ion source was accelerated by –13 kV at the source with total impact energy of 23 keV to sample surface (+10 kV sample voltage).

In S1 and S2, primary beam was set to 10 nA and 1.6 nA, respectively, and rastered over 25 μm and 10 μm areas that helped in maintaining the stability of secondary ions. The higher intensity analyses (S1) were for glass with low TiO_2 contents 0.02-0.3%, while session S2 was

for TiO_2 from 0.3 to 3%. The secondary $^{47}Ti^+$ intensity was in the range from 7×10^3 to 2×10^5 cps. Dead time of the EM pulse counting system is 23 ns, which is determined electronically by the counting system. Total 120 and 100 cycles were collected in S1 and S2, respectively, with the total analysis time of 40-50 minutes. In S2, secondary ion intensities change more rapidly, so the isotope ratios were calculated by applying linear drift correction.

In S3, primary beam was set to 40 nA with raster size of 15 μm. The $^{47}Ti^+$ and $^{49}Ti^+$ ions were detected using two FCs on the multicollection system. The secondary $^{47}Ti^+$ intensities were ~5×10^6 cps for glass with 3% TiO_2. Each analysis consists of presputtering (60 s), secondary ion centering, and 200 s acquisitions of Ti isotopes (4s × 50 cycles) with total analysis time of 6 minutes. These detectors employed high gain 10^{12} ohm feedback resistors (Fukuda et al. 2021), which reduce thermal noise down to ±200 cps levels compared to those with 10^{11} ohm resisters and allowed us to analyze Ti isotopes using 2 FCs at the intensities down to a few $\times10^5$ cps.

(2) For reducing matrix effect in measuring due to chemical composition variation along the diffusion profile, we prepared sample HB30 by ½-inch piston-cylinder apparatus at the University of Michigan. HB30 has the same original $^{49}Ti/^{47}Ti$ ratio as the couple by using same reagent chemicals but with a TiO_2 concentration of 0.27 wt%, between that on the high Ti and low-Ti sides of the couple to match intermediate compositions along the diffusion couple. In S1 and S2, this sample was repeatedly analyzed during the analyses of the experimental samples to monitor the possible data drift. And HB30 analyses were reproducible within 0.4-0.5‰ that are similar to the internal uncertainties.

The titanium isotope ratio is expressed using the δ-notation as follows:

$$\delta 49Ti = \left(\frac{(49Ti/47Ti)_{sample}}{(49Ti/47Ti)_{standard}} - 1\right)1000‰, \quad (5)$$

where $(^{49}Ti/^{47}Ti)_{sample}$ is the ratio measured at a given point in the sample, and $(^{49}Ti/^{47}Ti)_{standard}$ is the ratio in the standard (Leya et al. 2007; Niedere et al. 1981). There is no need to obtain the absolute isotope ratio when determining β value, the relative value is enough (Zhang, 2022). In S3, analyses of high TiO_2 end of experimental sample ($x \geq 700$ μm from the boundary) was repeatedly analyzed four times between ~10 unknown analyses (an example of HB17&18A shown in Fig.2a). The external reproducibility of $x \geq 700$ μm data were better than 0.2‰ (2SD) and are consistent with the source material HB18 glass in a different mount (raw $^{49}Ti/^{47}Ti$ ratio is -14.90 ± 0.07‰ from this analyze). Hence, $(^{49}Ti/^{47}Ti)_{standard}$ taken to be the ratio at the high-TiO_2 concentration.

Chapter 3 Result

The SIMS data provide both $^{49}Ti/^{47}Ti$ isotope ratios and ^{47}Ti counting rate. To convert the counting rate profile to concentration profile, ^{47}Ti counting rate is normalized by the internal standard $^{30}Si^{16}O$ to remove effect of beam fluctuation and other instrumental variation. For the diffusion couple HB17&18A, because SiO_2 concentration is essentially constant, the $^{47}Ti/^{30}Si^{16}O$ ratio at a given point is proportional to TiO_2 concentration. Hence, using electron microprobe data at high-Ti side as calibration, the TiO_2 concentration can be calculated. For S1, S2, and S3 segments, concentrations were made consistent by moving the profile of a segment up and down until they match. However, for HB11&12F diffusion couple, SiO_2 concentration varies along the profile. TiO_2 concentration in S1 and S2 session are obtained by the $^{47}Ti/^{30}Si^{16}O$ ratio and HB11&12F is a Si-Ti couple, which means we need to correct Si concentration on every data point. We use the Si diffusivity from Guo and Zhang (2016) to determine the true SiO_2 concentration. After that, the concentration profiles of two samples from SIMS are in general

consistent with EMPA data. Another trouble on HB11&12F (Fig.1b) is that it has a horizontal crack near the interface. The distance across the crack is corrected using the same correction as in Guo and Zhang (2016).

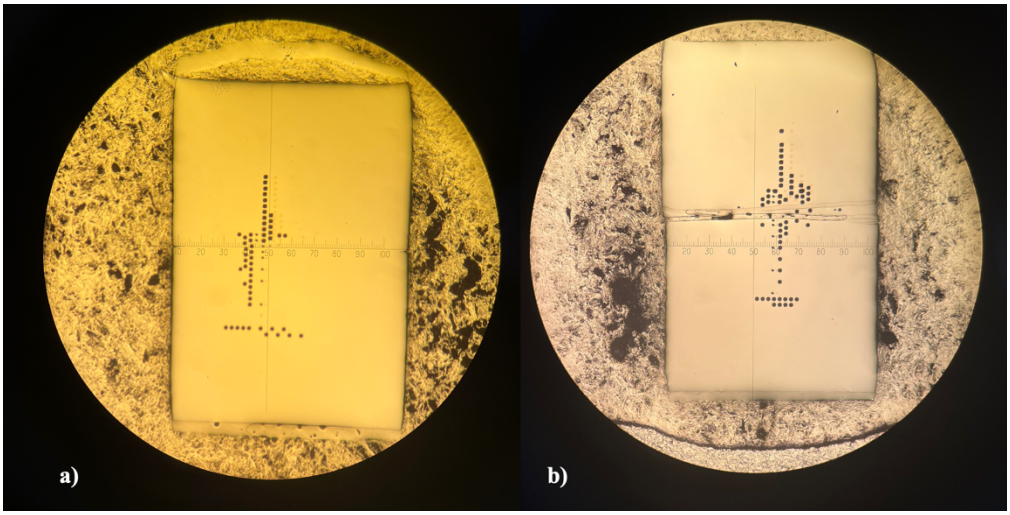

Fig.1 microscope photos of a) HB17&18A and b) HB11&12F after SIMS analysis. Different analyze session use different spot size (width (μm) × height (μm)) and shape: 34 × 28 rectangle (S1), 21 × 12 triangle (S2) and 35 × 27 oval (S3).

3.1 $(^{49}Ti/^{47}Ti)_{standard}$ for the profile

S1, S2 and S3 are in different analytical condition, the raw isotope ratio (using literature standard as $(^{49}Ti/^{47}Ti)_{standard}$) will difference even though on the same position (Fig.2a). Therefore, we need to connect the $\delta^{49}Ti$ result of these three sessions. As we discussed before, the ratio on high-TiO_2 concentration side is used as the standard in this study because we are only interested in relative $^{49}Ti/^{47}Ti$ isotope variations. For S2 and S3, we can directly use the average $\delta^{49}Ti$ of high concentration side on each session. However, there is no data on high-TiO_2 concentration side for S1. We move the whole segment up or down until the overlapping profiles become consistent (Fig.2b). About newly introduced errors during connecting profile, we use standard

error of points we chose before for S2 and S3 and 0.2 ‰ for S1 by considering visual matching error.

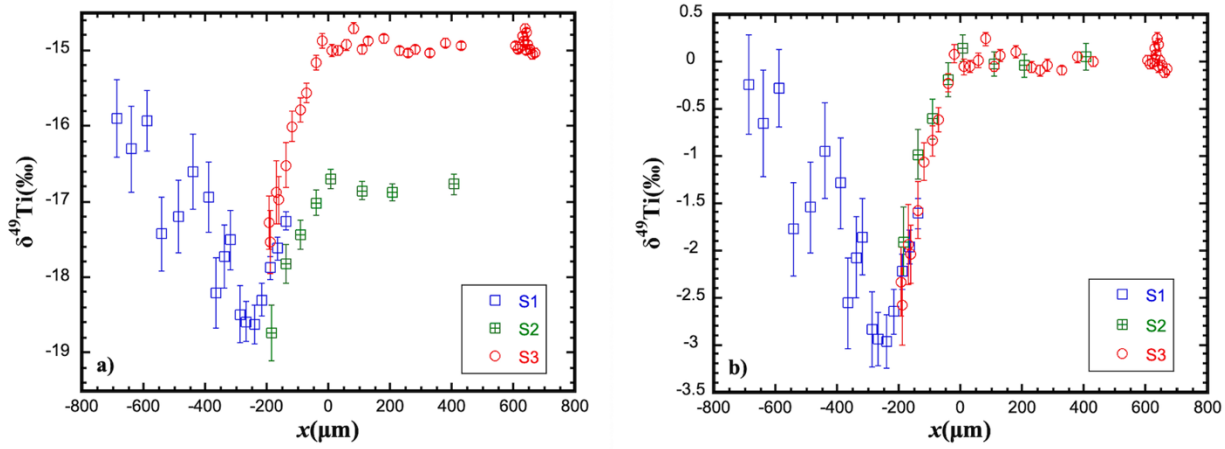

Fig.2 δ^{49}Ti ratio for HB17&18A using a) literature absolute ratio standard; b) average high-TiO_2 concentration side as standard and matching data to obtain consistency.

3.2 ^{49}Ti/^{47}Ti isotope ratio profiles

^{49}Ti/^{47}Ti profiles of two samples are shown in Fig.2 and Fig.3, together with TiO_2 concentration profiles for comparison. The small maximum ^{49}Ti value is shown on the high-TiO_2 concentration side and the large minimum ^{49}Ti value is occurred on the low-TiO_2 concentration side. And the position of maximum is nearer to interface compared to the minimum. This is because ^{49}Ti has larger mass and less diffusivity than ^{47}Ti. Hence, at the high-TiO_2 concentration side, ^{47}Ti is faster to low concentration side, leading to a maximum in δ^{49}Ti. At the low-TiO_2 concentration side, there is extra ^{47}Ti, leading to a minimum in δ^{49}Ti, and due to the larger diffusivity, the peak of minimum in δ^{49}Ti will be further to interface than the maximum.

Chapter 4 Discussion

4.1 Modeling the TiO_2 and $^{49}Ti/^{47}Ti$ diffusion profiles

Although there is multicomponent diffusion happening in these diffusion couples, we firstly assumed constant EBDC (effective binary diffusion coefficients) values to model the TiO_2 and $^{49}Ti/^{47}Ti$ diffusion profiles due to TiO_2 is the composition which has main concentration gradient in these couples. In this assumption, the concentration profiles of ^{49}Ti and ^{47}Ti would be error function; therefore, the isotope ratio $^{49}Ti/^{47}Ti$ can be expressed as follows:

$$\frac{49Ti}{47Ti} = \frac{0.5\left(C_{49,LHS} + C_{49,RHS}\right)+0.5\left(C_{49,RHS} - C_{49,lHS}\right)\frac{x-x_0}{\sqrt{4D_{49}t}}}{0.5\left(C_{47,LHS} + C_{47,RHS}\right)+0.5\left(C_{47,RHS} - C_{47,lHS}\right)\frac{x-x_0}{\sqrt{4D_{47}t}}}, \quad (6)$$

Where x_0 is the interface position, x increases from LHS to RHS, and subscripts 49 and 47 mean ^{49}Ti and ^{47}Ti. Transferring to the δ-notation and using the initial ratio at the RHS (high-TiO_2 concentration side) as standard lead to (Zhang, 2022):

$$\delta 49Ti = \{\frac{\left[\left(1+\delta_{LHS}\right)+R\right]+\left[R-\left(1+\delta_{LHS}\right)\right]\frac{x-x_0}{\sqrt{4(m_{47}/m_{49})^{\beta}D_{47}t}}}{[1+R]+[R-1]\frac{x-x_0}{\sqrt{4D_{47}t}}} - 1\}1000‰, \quad (7)$$

where $R = C_{RHS}/C_{LHS}$ is the initial concentration ratio of the RHS to the LHS which is determined accurately from the SIMS analysis and δ_{LHS} is $\delta^{49}Ti$ at the initial LHS which also needs to be modeled.

Constant EBDC assumption for TiO_2 in this study seems fitting TiO_2 concentration well for both SIMS and EMPA data (Guo and Zhang, 2016). The fitting for sample HB17&18A shown on Fig.3a can be an example. For the isotope profiles, constant EBDC also fit it well (Fig.3b) and the diffusivity modeled from concentration profile and isotope profile is consistent within error, only slightly difference. This consistent indicates that diffusion coefficients for TiO_2 on silicon melt has less relationship with its own concentration, which is not like the result on K isotope fractionation modelling (Zhang, 2022).

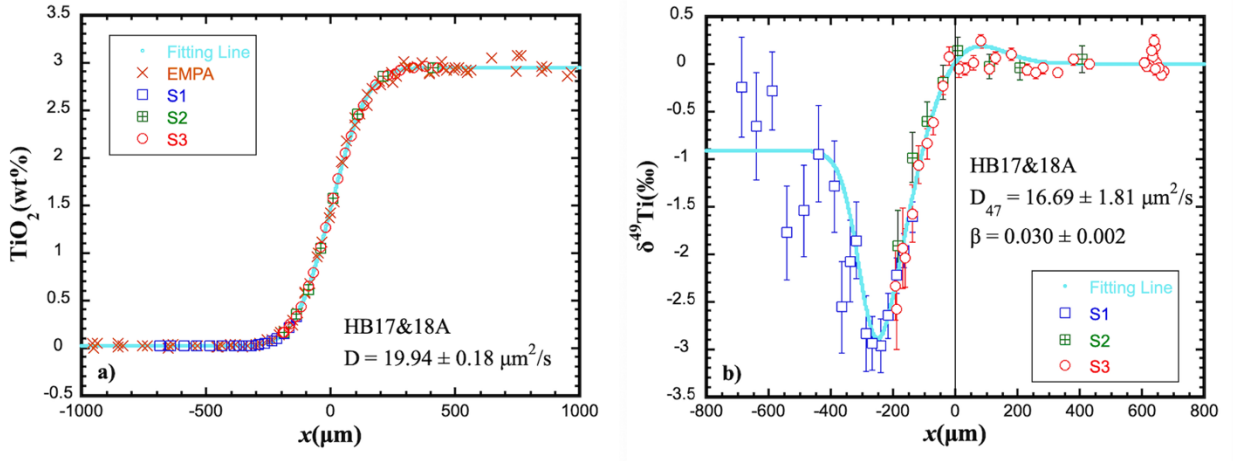

Fig.3 (a) Concentration and (b) isotope ratio profiles fit using EBDC for HB17&18A. Isotope ratio data show 1SD error. Where D means Ti diffusivity from concentration profile, D_{47} means ^{47}Ti diffusivity from isotope profile, black solid line shows modelled interface position (x = -4.63μm).

The fitting result of β value in this study is 0.030 ± 0.002 for the MgO-TiO_2 interdiffusion couples (Fig.3b) and 0.036 ± 0.004 for the SiO_2-TiO_2 interdiffusion couples (Fig.4b), which are close, indicating the similar mechanism. Here we try to explore the exchanging diffusion mechanisms in Ti isotope diffusion by using Eq.3 to determine clusters with target isotopes and counter-diffusing species. For diffusing species for titanium, one may first try TiO_2. However, the molecular mass for counter-diffusing species would be 11 to 9 amu for MgO-TiO_2 and SiO_2-TiO_2 couples respectively to produce the required β value, when combining Eq.1 and Eq.5,

which is much less than the mass for these two elements. If we constrain the counter-diffusing species to the simplest component (MgO and SiO_2) in these two couples, the nearest result of Ti component is $CaTiO_3$ ($\beta = 0.040$ for MgO-TiO_2), however, the result for SiO_2-TiO_2 is much larger than the fitting ($\beta = 0.054$). Through calculation, one of possible mechanisms to match the β value is $CaTiSiO_5$-$MgSiO_3$, where $\beta = 0.038$, matching both empirical β value and the similar mechanism hypothesis. In these two couples, CaO uphill diffusion from high to low TiO_2 concentration side are shown (Guo and Zhang, 2016), which would be evidence for calcium-titanium compound as cluster because it means Ca will diffuse accompanying with Ti even though reverse concentration gradient for Ca. However, the net flux of Ca is much less than Ti in these couples, indicating there may be mixing mechanisms in Ti isotope diffusion.

4.2 Isotope profile fitting for SiO_2-TiO_2 interdiffusion

For isotope profile of HB11&12F, convergence of fitting turned out to be difficult. The fitting result for this sample shown in Fig.4. Newton Method with Eq.7 which be used on HB17&18A shows bad simulation result on both diffusivity and interface position. We change to use Marquardt Method to obtain unique solution, which shows close EBDC with MgO-TiO_2 interdiffusion. However, the simulated interface position still has large distance with interface position modelled by TiO_2 concentration profile (near $x = 0$). The reason may firstly be the relatively large error on δ^{49}Ti value on low concentration part. For relatively low TiO_2 concentration of 0.015 wt%, the precision in measured $^{49}Ti/^{47}Ti$ is about 1.0‰ by single collection electron multiplier with magnetic field scan, which is much larger than Faraday cup data. One evidence of this explanation is that the fitting line leads to convergence even with Newton Method when a trial fit with reduced error on δ^{49}Ti value in low Ti concentration side. In

addition, it may also be due to uncertainties in visually fitting traverse S1 data into other data (details on Section 3.1). The large deviation produced when simulating the interface position further makes the final fitting curve does not match the data well and the larger error on other parameters. Therefore, continuous analysis of this sample with some new adjustments on our SIMS methods need to be done in the future.

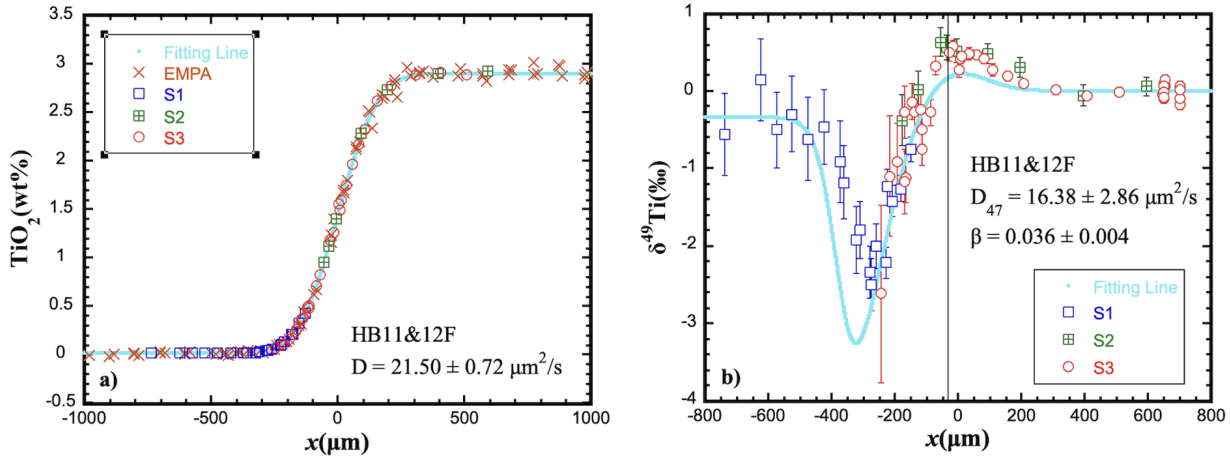

Fig.4 (a) Concentration and (b) isotope ratio profiles fit using EBDC for HB11&12F. Isotope ratio data also show 1SD error. D and D_{47} is same concept with Fig.2, and modelled interface position (x = -76.76μm) obviously deviates from the physical interface.

4.3 Relationship between diffusivity and β factors

Watkins et al. (2017) shows a possible relationship between β factors and the solvent-normalized diffusivity (D_i/D_{Si}, where i is the element for which diffusive isotope fractionation is considered). Now, we plot our new data of β with literature data from Watkins et al. (2017), Holycross et al. (2018) and Zhang (2022) on Fig.5. Being a high-field strength element, Ti diffusivity is not much different from that of Si in the melt; therefore, β factors close to 0 is expected and our result satisfied this correlation. However, there are plenty of β values ranging from 0.03 to 0.12 for different elements in the narrow range of diffusivity ratio between 1 and 2, indicating large uncertainty of the correlation. Considering these elements are all major

oxides in silicate melt, it may be necessary to use diffusion matrix treatment (Guo and Zhang, 2016, 2018, 2020). However, the available theory for diffusion matrix treatment for isotope fractionation during multi-component diffusion (Watkins et al., 2014) has too many isotope diffusion parameters and too difficult to apply.

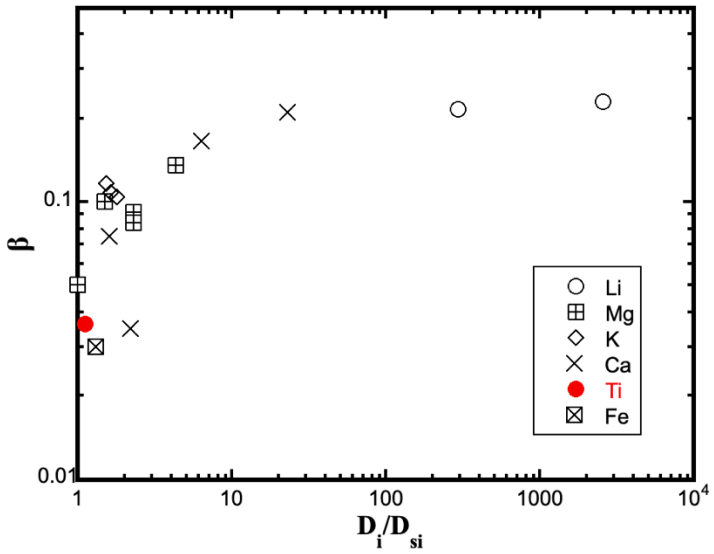

Fig.5 The relation between β_i factor and D_i/D_{Si}. β values for Ti (red solid circle) are from this work for the HB11&12F, the D_{Ti} and D_{Si} are from Guo and Zhang (2016) (D_{Si} values are not available for the HB17&18A). Other β values (black symbols) are from literature (Richter et al., 2003, 2008, 2009a; Watkins et al., 2009, 2011, 2017; Holycross et al., 2018; Zhang, 2022).

4.4 Diffusive Ti isotope fractionation during magmatic processes

Considering relatively small β factor for Ti, whether diffusive Ti isotope fractionation could be observed in nature magma system need to be discussed. From Eq.7, we know the diffusive isotope fractionation will be larger when increasing initial concentration ratio (defined to be $C_{TiO2,\ high}/C_{TiO2,\ low}$). Therefore, basalt-rhyolite magma mixing may lead to measurable diffusive Ti isotope fractionation. A rhyolite melt often contains relatively lower TiO_2, for example, 0.05 to 0.10 wt% (Nicholson and Shirey, 1990; Bloch et al., 1998) and a basalt melt may contain 1 to 5 wt% TiO_2 (e.g., Gale et al., 2013; Ayalew and Yirgu, 2003). Mixing of such

two melts would have an initial TiO_2 concentration ratio of 10 to 100. To simulate the isotope fractionation, the initial Ti isotopes in both melts are assumed to be the same with $\delta^{49}Ti = 0$. The EBDC of Ti is expected to be variable due to the compositions of the two melts to be mixed. There might also be uphill diffusion (Sato, 1975; Watson, 1982; Zhang et al., 1989), which must be treated using a multi-component diffusion approach. For simplicity, these two factors are ignored and the constant D from this study is used. The empirical fractionation parameter β is taken to be 0.030 based on this work (Fig. 3).

Fig.6 shows some simulation results for $^{49}Ti/^{47}Ti$ fractionation in magma mixing. The maximum $\delta^{49}Ti$ is less than 0.2‰ above the initial $\delta^{49}Ti$, which is difficult to resolve in nature. The minimum $\delta^{49}Ti$ is fairly significant, ≥1.5‰ lower than the surrounding $\delta^{49}Ti$ if the initial concentration ratio is greater than 50. This minimum occurs at $x/(4Dt)^{1/2} \approx 1$, and the exact position depends on the concentration ratio. One thing needs to be mentioned is that cooling might happen during magma mixing, meaning that diffusivity may depend on time. In such cases, (Dt) in Fig.6 should be replaced by $\int Ddt$, the integration of D with respect to time (Zhang, 2008). In natural samples, the presence of local $\delta^{49}Ti$ minimum shown in Fig.6 would be shown on phenocrysts or crystals growing in the local melt.

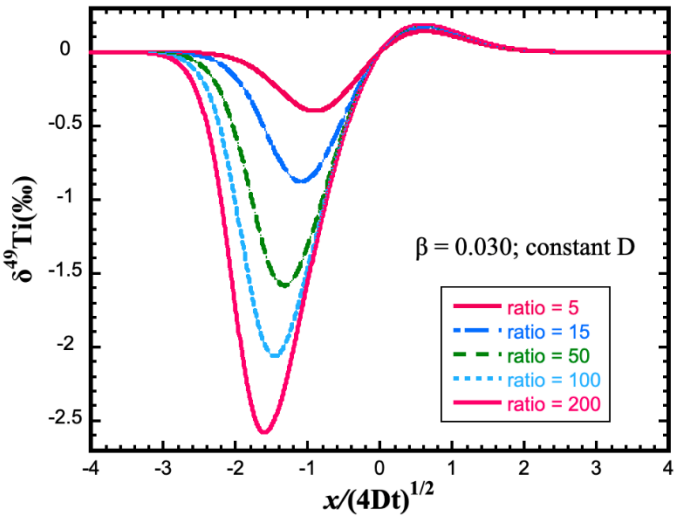

Fig.6 Simulated diffusion-generated δ^{49}Ti profiles. From left to right, the Ti concentration increase. In the simulation, β is taken to be 0.030 from result of Mg-Ti couple, D_{Ti} is taken to be constant, and initial δ^{49}Ti is zero in both low-Ti and high-Ti side. Different curves are for different initial concentration ratios. The horizontal axis is the normalized distance.

The isotope ratio peak on Fig.6 could also be recorded by other magma process such as melt percolating, which means the diffusion between melt and wall rocks. There is an example from Anguelova et al. (2022). They studied Ti isotope on Horoman orogenic peridotite massif on Hokkaido, Japan and found relatively high δ^{49}Ti value on parts of plagioclase-lherzolites and exceptionally low δ^{49}Ti value on some harzburgites and lherzolites (Fig. 7), comparing to other literature data (e.g, Millet et al., 2016) which is near 0.

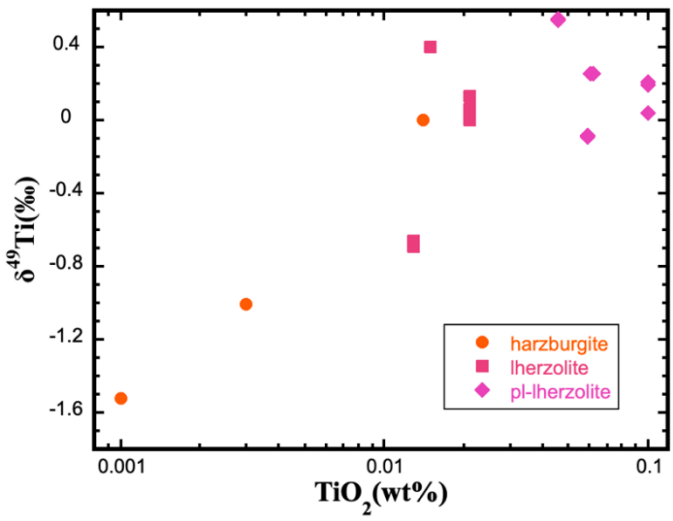

Fig.7 Titanium isotope data of the Horoman peridotites versus TiO_2 contents from Anguelova et al. (2022), and uncertainties (2SD) are smaller than symbol size. It shows that there is observable Ti isotope anomaly on low-Ti concentration part, which is consistent with the diffusive isotope fractionation we report here.

From the petrology study, this massif was affected by at least two distinct metasomatic events (Yoshikawa and Nakamura, 2000). Considering the high δ^{49}Ti value on crust composition (e.g., 0.184 ± 0.069 ‰ from Greber et al., 2017a), the high δ^{49}Ti value on plagioclase-lherzolites can be explained by metasomatism of the mantle wedge above the subduction zone. However, it is difficult to explain samples' low δ^{49}Ti by simply metasomatism of low δ^{49}Ti value melt/fluid due to 1) there is no exactly origin for this kind of melt/fluid on this environment; 2) the negative fractionation (nearly 1.5‰) is much larger than normal equilibrium ^{49}Ti/^{47}Ti fractionation from literature (e.g., about 0.6‰ for total δ^{49}Ti/^{47}Ti variation from Greber et al., 2021).

From Fig.6, we will find that this kind of variation could be achieved by diffusion. To obtain low δ^{49}Ti feature, there may be a melt containing high-Ti concentration to contact and diffuse with the harzburgites and lherzolites, but the melt only stayed for relatively short time to not reach equilibrium. Plagioclase-lherzolites seemly were not affected by this diffusion process, which means harzburgites and lherzolites with low δ^{49}Ti retained this ratio for long term and did

not expand to further end of the massif; therefore, closure temperature of Ti might be reached before low $\delta^{49}Ti$ signature across a greater volume of peridotite. For the minimum $\delta^{49}Ti$ of harzburgite (-1.5‰), the concentration contrast may at least be 50 from Fig.6; therefore, the concentration of the melt is nearly 0.1 wt%, which is consistent with lherzolites data (-0.2‰ variation to concentration contrast of 5). Due to the diffusivity is decrease with the time, the contrast needs to be increased, however, it may still be possible for some basalt melts or even rhyolite melts as we discussed before. Combining the previous research of $\delta^{7}Li$ anomaly by diffusion of the same massif (Lai et al., 2015), we are confident about our hypothesis which diffusion happen on the $^{49}Ti/^{47}Ti$ fractionation process.

Chapter 5 Conclusion

This study reports diffusive Ti isotope fractionation profiles in Si-Ti and Mg-Ti diffusion couples in multicomponent diffusion experiments of Guo and Zhang (2016). The initial concentration ratio between high-TiO_2 side and low-TiO_2 side is about 200. The total $^{49}Ti/^{47}Ti$ isotope ratio variation in these couples is near 3.5‰, which is much larger than equilibrium Ti fractionation on magma. The empirical isotope fractionation parameter β is found to be about 0.030 for the Mg-Ti series and 0.036 for Si-Ti series with concentration-independent effective binary diffusivity. The β value don't show large variation with different inter-diffusive element and is consistent with the empirical relation between β and ratio of diffusivity of the element to that of Si. The total Ti isotope ratio variation would be measurable when the initial TiO_2 concentration contrast is large enough (variation is > 1.5‰ when concentration contrast is ~50). Diffusive Ti isotope fraction can be used to explain the large Ti isotope fractionation on magma systems, especially negative anomaly, and further increasing understanding on magmatic processes, including tracing processes such as magma mixing and crystal growth, and inferring reaction and cooling time scales.

Bibliography

Anguelova, M., Fehr, M.A., Takazawa, E., Schönbächler, M., 2022. Titanium isotope heterogeneity in the Earth's mantle: A case study of the Horoman peridotite massif. Geochim. Cosmochim. Acta 335, 356-368.
Ayalew, D., Yirgu, G., 2003. Crustal contribution to the genesis of Ethiopian plateau rhyolitic ignimbrites: basalt and rhyolite geochemical provinciality. J. Geol. Soc. 160 (1), 47-56.
Bloch, J., Hutcheon, I.E., de Caritat, P., 1998. Tertiary volcanic rocks and the potassium content of Gulf Coast shales—The smoking gun. Geology. 26 (6), 527-530.
Chopra, R., Richter, F.M., Watson, E.B., Scullard, C.R., 2012. Magnesium isotope frac-tionation by chemical diffusion in natural settings and in laboratory analogues. Geochim. Cosmochim. Acta 88, 1-18.
Fortin, M.-A., Watson, E.B., Stern, R., 2017. The isotope mass effect on chlorine diffusion in dacite melt, with implications for fractionation during bubble growth. Earth Planet. Sci. Lett. 480, 15-24.
Fukuda K, Brownlee D. E., Joswiak D. J., Tenner T. J., Kimura M., and Kita N. T., 2021. Correlated isotopic and chemical evidence for condensation origins of olivine in comet 81P/Wild 2 and in AOAs from CV and CO chondrites. Geochim. Cosmochim. Acta 293, 544-574.
Gale A., C. A. Dalton, C. H. Langmuir, Y. Su, and J.‐G. Schilling (2013), The mean composition of ocean ridge basalts, Geochem. Geophys. Geosyst., 14, 489-518.
Greber, N.D., Pettke, T., Vilela, N., Lanari, P., Dauphas, N., 2021. Titanium isotopic compositions of bulk rocks and mineral separates from the Kos magmatic suite: Insights into fractional crystallization and magma mixing processes. Chem. Geol. Volume 578, 120303.
Greber N. D., Dauphas N., Bekker A., Ptáček M. P., Bindeman I. N. and Hofmann A. (2017a) Titanium isotopic evidence for felsic crust and plate tectonics 3.5 billion years ago. Science 357, 1271-1274.
Guo, C., Zhang, Y., 2016. Multicomponent diffusion in silicate melts: SiO2-TiO2-Al2O3-MgO-CaO-Na2O-K2O system. Geochim. Cosmochim. Acta 195, 126-141.
Guo, C., Zhang, Y., 2018. Multicomponent diffusion in basaltic melts at 1350◦C. Geochim. Cosmochim. Acta228, 190-204.
Guo, C., Zhang, Y., 2020. Multicomponent diffusion in a basaltic melt: temperature dependence. Chem. Geol. 549, 119700.
Holycross, M.E., Watson, E.B., Richter, F.M., Villeneuve, J., 2018. Diffusive fractionation of Li isotopes in wet, highly silicic melts. Geochem. Persp. Lett. 6, 39-42.
Huang, F., Lundstrom, C.C., Glessner, J., Ianno, A., Boudreau, A., Li, J., Ferre, E.C., Marshak, S., DeFrates, J., 2009. Chemical and isotopic fractionation of wet andesite in a temperature gradient: experiments and models suggesting a new mechanism of magma differentiation. Geochim. Cosmochim. Acta 73, 729-749.
Huang, F., Chakraborty, P., Lundstrom, C.C., Holmden, C., Glessner, J.J.G., Kieffer, S.W., Lesher, C.E., 2010. Isotope fractionation in silicate melts by thermal diffusion. Nature 464, 396-401.
Jambon, A., 1980. Isotopic fractionation: a kinetic model for crystals growing from magmatic melts. Geochim. Cosmochim. Acta 44, 1373-1380.

Lai Y.-J., von Strandmann P. A. P., Dohmen R., Takazawa E. and Elliott T. (2015) The influence of melt infiltration on the Li and Mg isotopic composition of the Horoman Peridotite Massif. Geochim. Cosmochim. Acta 164, 318-332.
Leya I., Schönbächler M., Wiechert U., Krähenbühld U., Halliday A. N., 2007. High precision titanium isotope measurements on geological samples by high resolution MC-ICPMS. International Journal of Mass Spectrometry 262, 247-255.
Millet M.-A., Dauphas N., Greber N. D., Burton K. W., Dale C. W., Debret B., Macpherson C. G., Nowell G. M. and Williams H. M. (2016) Titanium stable isotope investigation of magmatic processes on the Earth and Moon. Earth Planet. Sci. Lett. 449, 197-205.
Nicholson, S.W., Shirey, S.B., 1990. Midcontinent rift volcanism in the Lake Superior Region: Sr, Nd, and Pb isotopic evidence for a mantle plume origin. J. Geophys. Res. 95, 10851.
Nierdere F. R., Papanastassiou D. A., Wasserburg G. J., 1981. The isotope composition of titamium in the Allende and Leoville meteorites. Geochim. Cosmochim. Acta 45, 1017-1031.
Richter, F.M., Liang, Y., Davis, A.M., 1999. Isotope fractionation by diffusion in molten oxides. Geochim. Cosmochim. Acta 63, 2853-2861.
Richter, F.M., Davis, A.M., DePaolo, D.J., Watson, E.B., 2003. Isotope fractionation by chemical diffusion between molten basalt and rhyolite. Geochim. Cosmochim. Acta 67, 3905-3923.
Richter, R.M., Watson, E.B., Mendybaev, R.A., Teng, F.Z., Janney, P.E., 2008. Magnesium isotope fractionation in silicate melts by chemical and thermal diffusion. Geochim. Cosmochim. Acta 72, 206-220.
Richter, F.M., Watson, E.B., Mendybaev, R.A., Dauphas, N., Georg, B., Watkins, J.M., Valley, J.W., 2009a. Isotopic fractionation of the major elements of molten basalt by chemical and thermal diffusion. Geochim. Cosmochim. Acta 73, 4250-4263.
Richter, F.M., Watson, E.B., Chaussidon, M., Mendybaev, R., Christensen, J.N., Qiu, L., 2014. Isotope fractionation of Li and K in silicate liquids by Soret diffusion. Geochim. Cosmochim. Acta 138, 136-145.
Richter, F.M., Mendybaev, R.A., Christensen, J.N., Hutcheon, I.D., Williams, R.W., Sturchio, N.C., Beloso, J., A.D., 2006. Kinetic isotopic fractionation during diffusion of ionic species in water. Geochim. Cosmochim. Acta 70, 277-289.
Sato, H., 1975. Diffusion coronas around quartz xenocrysts in andesite and basalt from Tertiary volcanic region in northeastern Shikoku, Japan. Contrib. Mineral. Petrol.50, 49-64.
Watkins, J.M., DePaolo, D.J., Watson, E.B., 2017. Kinetic fractionation of non-traditional stable isotopes by diffusion and crystal growth reactions. Rev. Mineral. Geochem.82, 85-125.
Watkins, J.M., DePaolo, D.J., Huber, C., Ryerson, F.J., 2009. Liquid composition-dependence of calcium isotope fractionation during diffusion in molten silicates. Geochim. Cosmochim. Acta 73, 7341-7359.
Watkins, J.M., DePaolo, D.J., Ryerson, F.J., Peterson, B.T., 2011. Influence of liquid structure on diffusive isotope separation in molten silicates and aqueous so-lutions. Geochim. Cosmochim. Acta 75, 3103-3118.
Watkins, J.M., Liang, Y., Richter, F., Ryerson, F.J., DePaolo, D.J., 2014. Diffusion of multi-isotopic chemical species in molten silicates. Geochim. Cosmochim. Acta 139, 313-326.
Watkins, J.M., DePaolo, D.J., Watson, E.B., 2017. Kinetic fractionation of non-traditional stable isotopes by diffusion and crystal growth reactions. Rev. Mineral. Geochem.82, 85-125.

Watson, E.B., 1982. Basalt contamination by continental crust: some experiments and models. Contrib. Mineral. Petrol.80, 73-87.
Yoshikawa M. and Nakamura E. 2000 Geochemical evolution of the Horoman peridotite complex: Implications for melt extraction, metasomatism, and compositional layering in the mantle. J. Geophys. Res. (Solid Earth) 105, 2879-2901.
Zhang, Y., 2022. Diffusive fractionation of K isotopes in molten basalts. Earth Planet. Sci. Lett. 581, 117405.
Zhang, Y. and Gan, T., 2022 Diffusion in Melts and Magmas. Rev Mineral Geochem. 87 (1), 283–337.
Zhang, Y., Walker, D., Lesher, C.E., 1989. Diffusive crystal dissolution. Contrib. Mineral. Petrol.102, 492-513.
Zhang, Y., 2008. Geochemical Kinetics. Princeton University Press, Princeton, NJ.